Draft version April 21, 2017
Preprint typeset using LaTeX style AASTeX6 v. 1.0

arXiv:1703.10022v3 [astro-ph.SR] 20 Apr 2017

A CORONAL BLOWOUT JET ASSOCIATED WITH A DOUBLE-CME AND SHOCK WAVE

Y. H. MIAO[1,2], Y. LIU[1], Y. D. SHEN[1], A. ELMHAMDI[3], AND A. S. KORDI[3]

[1]Yunnan Observatories, Chinese Academy of Sciences, Kunming 650011, China
[2]University of Chinese Academy of Sciences, Beijing 100049,People's Republic of China
[3]Department of Physics and Astronomy, King Saud University, PO Box 2455, Riyadh 11451, Saudi Arabia

ABSTRACT

Based on high-resolution *Big Bear Solar Observatory* (*BBSO*), *Solar Dynamics Observatory* (*SDO*) and *Solar Terrestrial Relations Observatory* (*STEREO*) data, AR NOAA 11166 (on March 09, 2011) is found to be the theater of a small Hα filament eruption during a blowout jet phase, whose length is estimated to be larger than 400 Mm with an average velocity of about 270 km s^{-1}. An evident magnetic flux cancellation is observed on the photosphere during the double-CME blowout jet. The blowout jet is found to show an unwinding motion during the eruption phase. Interestingly, using *SDO*/AIA 193 Å observations, a short time shock wave is reported at the beginning of the eruption. From sl SDO viewpoint, the bubble-like CME was formed by the front part of the jet, while the jet-like CME was formed by the rectilinear part of the jet. Additionally, from *STEREO* COR1 A and B viewpoints, an overlapping of the two CMEs were due to the special magnetic field distribution on the photosphere that we depict in a simple sketch model. The studied event, blowout jet with two simultaneous CMEs, with its atypical structures indicates again that a variety of solar activities with different spatial scales might simultaneously take place and integrate into one solar eruption phenomenon.

Keywords: Sun: activity — Sun: filaments — Sun: jet — Sun: coronal mass ejections (CMEs) — Sun: — flare

1. INTRODUCTION

Jet activities are recurring phenomena in the solar atmosphere, which have been well studied over the last few decades. Coronal jets are often associated with hot plasma being ejected from the chromosphere into the solar corona. In UV or EUV wavelengths they are directly called jets, while when occurring in X-ray wavelengths they are dubbed X-ray jets (Liu et al. 2015; Sterling et al. 2015; Shibata et al. 1992). UV, EUV and X-ray jets are associated with high-temperature plasma. When jets are observed in Hα wavelength, they are called surges, and they are believed to be the cool counterparts of the hot coronal jets. Additionally, Hα surges and UV, EUV or X-ray jets are found to be configured in a side-by-side geometry (Liu & Kurokawa. 2004; Shen et al. 2011). Over the last two decades many authors have shown great interest in studying various aspects of such events. Liu et al. (2005) introduced a surge-coronal mass ejection event, later Liu (2008) described a series of jet-like surges which were separately followed by one corresponding jet-like CME. According to more recent investigations, some solar active regions happen to be the site of multiple homologous jets, i.e. the so-called blowout jets (Shen et al. 2012; Chen et al. 2015; Li et al. 2015). The blowout jets, however, often result from small-scale filament eruptions accompanied by scenarios of transverse drifting and rotation (e.g., Moore et al. 2013; Zhang et al. 2016). In Cirtain et al. (2007) work, the authors observed a very active area, with a frequency of ten jet events per hour. Some models have been proposed to explain the standard jets and the blowout jets events (see Moore et al. 2010; Sterling et al. 2016 and references therein). The authors noticed and argued the standard jets spire to be narrow, while the blowout jets spire are broad. Admas et al. (2014) concluded that a small-scale feature seen in an erupting mini-filament may lead to jet eruption, and the absorption feature could perhaps be observed well in 304 Å . Shimojo et al. (1996, 1998) found that the blowout jets lengths to range from a few $\times$ 10^4 to 4$\times$ 10^5 km, while the widths should range from 5$\times$ 10^3 to 1$\times$ 10^5 km. Regardless of the nature of the cool plasma surges or the hot plasma jets, the events are possibly the same phenomenon but observed in different wavelength channels. Recently, the solar physics community showed considerable interests in exploring and scrutinizing both observationally and theoretically the triggering mechanisms behind jets and CMEs solar phenomena. Indeed

a series of papers were published dealing with this hot topic, illustrating and probing a variety of possible physical mechanisms (e.g., Chen et al. 2015; Liu et al. 2015; Sterling et al. 2015). Large limb jet events are often associated with obvious CMEs (Liu 2008). In fact in the cited paper it was found that all of the jet-like surges were associated with jet-like CMEs. Various types of jets in the solar atmosphere are crucial in promoting mass and energy conversion as well as in different spatial-temporal scales (e.g., Katsukawa et al. 2007; Murawski et al. 2011; Morton et al. 2012; Shen et al. 2011, 2012; Filippov et al. 2015). Jet-like surges have large-scale nature, and are relevant in the channeling of mass and energy into the upper corona (Murawski et al. 2011). Additionally, in the lower solar atmosphere, many types of jet-like surges appear at short temporal and spatial scales. Coronal and chromosphere jets are hot plasmas along open or large-scale magnetic field lines, with often linear or slightly bent structures (Shen et al. 2011). Some blowout jets can generate simultaneous bubble-like and jet-like CMEs (Shen et al. 2012). Independently of the scale at which the jets manifest (large or small), the basic mechanisms are considered to be due to magnetic reconnection and magnetohydrodynamic (MHD) wave activity, driving the heated plasma ejecta in the solar atmosphere (e.g., Liu & Kurokawa. 2004; Liu et al. 2005; Shen et al. 2011, 2012; Morton et al. 2012). Very recently, Alzate & Morgan (2016) observed a structure-less " PUFFS" jet eruption area followed by a slow coronal mass ejection. One jet eruption followed by one CME might be a common event. Another interesting recurrent blowout jets event had been presented and studied by Chen et al. (2015). Liu et al. (2015) indicated the coronal jets to be closely connected to the coronal CMEs. Other investigations interpret X-ray jets in solar coronal holes as due to the small-scale filament eruptions (Sterling et al. 2015). Some twisting jets formation might be in close conjunction with the filaments (Filippov et al. 2015). Moreover, there might be a strong association of jet events CMEs, with the large-scale jets being mostly the triggering mechanism of CMEs (Liu et al. 2015). Regardless of the involved mechanism of solar jets (cooling or heating), they still might be observed in multi-wavelengths. Generally, solar jets have relation with magnetic flux emergence and cancellation (Sterling & Moore. 2004; Liu et al. 2005). Solar surges may be triggered by impulsive generation of a pressure pulse (Shibata & Uchida. 1986), and may be also associated with explosive events (Madjarska et al. 2009). Up to now, there is still no distinct and clear observational research on CMEs that is combined with the coronal blowout jets. Moore et al. (2010) had pointed out that coronal jets might be observed in the outer corona. Coronal mass ejections(CMEs) usually have large scale magnetic structures, which can drive shocks in the corona and interplanetary space (Liu et al. 2017). Some shock waves were observed low in the solar atmosphere accompanied with CMEs. They dubbed these shock waves, EUV waves. EUV waves propagate at typical speeds of 200-400 km s^{-1} (Dissauer et al. 2016; Muhr et al. 2014)

In this paper, we present an intriguing case of a blowout jet event occurring in the NOAA AR11166 (N11W15) on 2011 March 09. Multi-wavelength data taken by Solar Dynamics Observatory (*SDO*), Solar Terrestrial Relations Observatory (*STEREO*), and Big Bear Solar Observatory (*BBSO*) are used. It must be pointed out that Shen et al. (2012) introduced the first double CMEs event however not as clear and evident as the studied case subject of the present paper. Special emphasis will be placed on the bubble-like CME and the associated jet-like CME. Additionally, using *SDO*/AIA 193 Å observations, we report the presence of a short time shock wave accompanying the filament eruption.

2. OBSERVATIONS AND DATA ANALYSIS

2.1. *Data*

The blowout jet, subject of the present work, leads conjointly to a bubble-like CME and a jet-like CME, that we dub here "simultaneous double-CME". The Hα full-disk data, from *BBSO* permit to recognize the blowout jet. The corresponding data have a pixel width of 1″ and a cadence of 1 minute. Next, we search through the high temporal and spatial resolution *SDO* data. The *SDO*/Helioseismic and Magnetic Imager (HMI; Scherrer et al. 2012) supplies full-disk line-of-sight (LOS) magnetograms at a pixel width of 0″.6 and a precision of 10 G with a 45 seconds cadence, while *SDO*/Atmospheric Imaging Assembly (AIA) has 12 seconds cadence and exposures of 0.12-2 seconds. The Sun's atmosphere is imaged out to 1.3 R$\odot$ in seven Extreme Ultraviolet (EUV) and three Ultraviolet (UV)-visible wavelength bands, with a similar pixel width to that of HMI. Among the seven EUV wavelength channels, 131 Å , 171 Å , 193 Å , 211 Å , 335 Å , and 94 Å , wavelengths are due to strong iron lines with temperature range from 0.6 MK to 16 MK. While *SDO* and *BBSO* observe the Sun from the viewpoint of Earth, the *STEREO* Ahead and Bhead observe the Sun from two other viewpoints. The Extreme Ultraviolet Imager (EUVI) of the Sun Earth Connection Coronal and Heliospheric Investigation (*SECCHI*) takes full-disk He II 304 Å images on board *STEREO* Ahead and Bhead. The 304 Å images have a 10 minutes cadence and a pixel width is 1″.6. COR1 and COR2 are on board *STEREO*-Ahead and Bhead which take images have a cadence of 5 minutes and the field view (FOV) from 1.4 to 4 R$\odot$.

The data from all three cited instruments are used in our present investigation.

2.2. *Shock Wave and Double CME*

Closely analaying *BBSO* Hα full-disk data, we were able to detect a small filament eruption and also a filament peculiar feature, by following similar description as in Admas et al. (2014). In Figure 1, we explore the *BBSO* data to underline the filament configuration ("F" symbol), and to figure out how the "F" feature forms and erpts. From (a) to (e), Figure 1, the appears to be the site of few jet eruptions. More details will be given and discussed later. From (f) to (k), we can clearly recognize the filament formation around 21:35 UT. In panel (l), at 22:05 UT, the blowout jet active region began to brighten, then followed by a flare event. Jet eruptions injected plasma into the corona that subsequently cools down leading to the filament formation. This eruption process is evidenced from the accompanying Hα movie (video1).

To probe more the configuration of the event, we use *SDO*/AIA 171 Å , 193 Å , and 304 Å channels as displayed in Figure 2. In top panel from (a) to (a2), we can distinguish the "F" feature, especially in 304 Å . From (b) to (b2), at about 22:05 UT, the feature started to erupt and the active area started to brighten, with the following jet having an untwisted motion. In the third and fourth panels, from (c) to (d2), the displayed series of images highlight the jet eruption process. Later on, at about 22:20 UT the jet appears to split into two parts, with the front part starting to move on. This stage is shown in the accompanying online material (video2).

In Figure 3, the vertical and horizontal dotted lines, at 22:14 UT-top panel, indicate the two paths along which the distance - time measurements have been made with *SDO*/AIA 171 Å data. The second panel shows the coronal jet where the distance is measured along the chosen slit, while in the bottom panel we mark the height of about 40 Mm across the jet. The second panel is mainly used to measure the blowout jet of the EUV wavelength bands. The maximum length was estimated to be about 400 Mm with an approximately maximum velocity of 350 km s^{-1}. In our work however the simultaneity of the jet-like and bubble-like CMEs appeared more pronounced and evident. Worth noticing here the paper by Liu (2008) treating Hα jet-like surges. The authors measured the maximum speeds and the maximum lengths and found values of 50-200 km s^{-1} and $(5-20) \times 10^4$ km, respectively. To understand the possible causes behind the differences between our event and the one of Liu (2008), we focus on the structure of the blowout jet. Figure 3 illustrates the distance - time image plot along the jet. In the top panel, the black dotted line indicates the trend along the jet. It should be noted that the jet scale was very large and long. In the bottom panel, we highlight the blowout jet and the height-time variation along the jet. We measured the front part velocity to be about 190 km s^{-1} and the bottom part velocity about 350 km s^{-1}. The extracted slit is almost 67 Mm length, and we only focused on the brighter area with a 40 Mm width. From Figure 3 (second and bottom panels), it was very evident that the jet scale was very large and the eruption was very intense, hence the necessity to further inspect the jet eruption area magnetic field.

Curiously, around 22:06 UT, we detect a shock wave from *SDO* 171 Å , 193 Å , and 211 Å images. We highlight it in a movie made by 193 Å difference images (video3). The wave was persistence about six minutes and then disappeared. The time was so short, but the shock wave profile could clearly and easily be distinguishable. From Figure 4 panel (a1) and (b1), we used 171 Å and 193 Å images to show the shock wave profile. Jet eruptions associated to shock waves were rarely observed in the past decades. At about 22:12 UT, a bubble-like CME and jet-like CME manifested. Panel (a2) and (b2) showed the bubble profile. We also present a movie using 193 Å difference images. Where the bubble profile was clearly seen. From *SDO* viewpoint the jet-like CME appeared above the bubble-like CME (see video4). From the Figure 3 middle panel, we measured the two-parts velocities, with the first part velocity estimated about 350 km s^{-1}. Interestingly, the shock wave appeared at the beginning eruption of the blowout jet, and the blowout jet just in the accelerated phase. From the shock movie (video3), we recognize a huge power at the moment of the blowout eruption.

In Figure 5 we display *SDO* 1600 Å , 1700 Å , 171 Å , and line of sight HMI images. Panel (a) to panel (c) show the HMI image overlaying AIA images at 22:04:59 UT. The blue line represents the negative magnetic field and red line represents the positive magnetic field. The contour levels are ±100, ±50 G. In panel (a), the "P", "N", "P1", denote the main positive magnetic field, emerging negative magnetic field and the open positive magnetic field, respectively. Panel (a) will be used to interpret the jet eruption model cartoon of Figure 10. Panel (b) shows three bright points: " A1", " A2", " A3". We select the three bright-point areas: $5'' \times 11''$ " A1", $10'' \times 9''$ " A2", $11'' \times 14''$ " A3", which are also counterpart of panel (d). In panel (c), we report the jet eruption in 171 Å wavelength at the beginning stage where we can also notice the intensity being greater than in 1600 Å and 1700 Å . Panel (d) shows the line-of-sight HMI image and three magnetic fields, which are the counterpart of the three bright-point areas of panel (b). The main purpose of the three selected areas of panel (d) were to calculate the negative magnetic flux variation.

Indeed, in Figure 6, we display the three areas flux variation curves. From top to bottom of Figure 6, the three panels correspond to " A1", " A2", " A3" magnetic fields flux variation curves from 21:31:14 UT to 22:38:44 UT, respectively. In top panel, the fast decline in the negative magnetic flux is indicative of the magnetic cancellation leading role in " A1". At 21:31:14 UT (X-axis=0), the negative flux was 5×10^{19} Mx, decreasing to a value around 3.3×10^{19} Mx at 22:00 UT, while at 22:15 UT it reached a flux about 2×10^{19} Mx. Hence, reduced by an amount of about 3×10^{19} Mx in less than two hours time inerval (i.e. from 21:31 UT to 22:15 UT), which might suggest a scenario of magnetic cancellation to occur during the blowout jet eruption stage. The " A2" negative flux evolution is highlighted in the middle panel. The curve shows a descending behaviour stage, from 21:31 UT to 22:00 UT, dropping by an amount of 1.5×10^{19} Mx, from about 3.7×10^{19} Mx to 2.5×10^{19} Mx, then it increased by about 0.7×10^{19} Mx in the time interval 22:05 UT to 22:30 UT. Interestingly, the flux evolution of " A2" might suggest that it was associated with flux emergence and magnetic cancellation during the blowout jet eruption stage. The bottom panel displays the " A3" flux variation. From 21:31 UT to 22:05 UT the negative flux appears to increase. Later on it shows an almost constant plateau phase (from 22:05 UT to 22:30 UT). The first stage had an increase amount of about 2.3×10^{19} Mx in the negative flux,evidencing that " A3" associated flux emergence might have played the leading role during the blowout jet eruption stage. According to Moore et al. (2010) and Moore et al. (2015), blowout jet eruption has complex field, associated with untwist motion. As the Figure 6 shows, " A1", " A2", " A3" magnetic emergence and cancellation generated an enormous amount of energy to lead to a so large scale blowout jet eruption. In addition, an C9.4 flare followed the blowout jet eruption during 22:05 UT to 22:12 UT, suggesting the jet eruption being very intense (see video2).

It should be noted that the three magnetic field areas have a very complex magnetic field structure and formation process (Figure 6), suggesting the jet eruption has accompanied local flux emergence and magnetic cancellation. Combining the above observations facts and analysis we conclude that the negative magnetic structure has been cancelled. Interestingly, a simultaneous jet-like and a bubble-like CMEs were observed to be associated with the blowout jet in the field of view (FOV) of the COR1 Ahead and COR1 Bhead of *STEREO*. The positions of COR1 Ahead and COR1 Bhead are shown in Figure 7. Fortunately, the *STEREO* two satellites have successfully photographed the blowout jet eruption. This stage is highlighted with a movie combining *STEREO* and *SDO* data (video5; the simultaneous jet-like and the bubble-like CMEs; provided with the online material). Using the 304 Å COR1 Ahead and COR1 Bhead images, we have further investigated the double CMEs event. The double simultaneous CMEs are shown in Figure 8. From the two viewpoints of *STEREO* satellite, we can observe the intriguing blowout jet and its different characteristics. Panels (a) and (b) show Ahead 304 Å images at 22:26 UT and 22:36 UT, respectively. Panel (c) and panel (d) report Bhead 304 Å images at the same time as panels (a) and (b). The second and third columns are for COR1 Ahead, COR1 Bhead images, respectively. Panels (b1) and (b2) indicate the bubble-like CME first reached the FOV of COR1 at about 22:25 UT. At around 22:40 UT, the jet-like CME was very clear, marked as a black arrow. We could clearly see and distinguish the arcus bubble-like CME. Panels (c1), (c2), (d1) and (d2) illustrate the double CMEs eruption process stages. Moreover, we report a series of videos (video6;video7,video8; online material), that help the reader easily recognize the two simultaneous CMEs.

3. DISCUSSION AND CONCLUSIONS

In the present study, we investigated the physical triggering mechanism of the blowout jet, observed in the active region NOAA 11166 on March 09, 2011 which associated a jet-like and a bubble-like CMEs, observed by *SDO*,*BBSO* and the COR1 on board *STEREO* Ahead and Behind. It is noted that a short time shock wave was detected during the beginning of the eruption. Jet eruptions associated to shock waves were rarely observed in the past decades, this event is of important significance in studying the solar physics in the future.

In order to understand the possible jet eruption mechanism at four critical moments, we sketch a two-dimensional cartoon model, highlighted in Figure 10, where only few representative field lines are drawn. Our proposed cartoon model, appears to be a combination of the standard jet model with the well-known flux rope eruption model (Lin & Forbes. 2000). The model-view illustrates some observable properties of the blowout coronal jets, involving the filament eruption, possibly revealing the nature of the simultaneous jet-like and the bubble-like CMEs. Note also that the principle triggering mechanism was similar to the Antiochos et al. (1999) model, namely, the magnetic breakout model. In addition, some characteristics were similar to what proposed by Liu et al. (2015) model, where the internal magnetic lines had a twist-wrap structure. The blowout jet with double CMEs events, might be attributed to a variety of solar activities with different physical mechanisms that can simultaneously take place, at large scale, and integrate into one solar eruption phenomenon. We present the double-CME event reveals many different

characteristics, namely: a) the jet scale was greater, making it more pronounced and intense. Indeed, our blowout jet was at least 4×10^5 km (600″) long and 40 Mm (nearly 100″) width. The jet two parts velocities are estimated to be 350 km s^{-1}, 190 km s^{-1} (Figure 3;b) a short time shock wave was observed. Indeed, the shock wave can be detected by *SDO*/AIA 171 Å , 193 Å and 211 ÅİIn Figure 4 panel (a1) and (b1), we indicated the shock wave profile. Jet eruptions associated to shock waves were rarely observed, this event maybe produce significant influence in the future; c) with two different observed views. The position of the AR 11166 and the *STEREO* twin spacecraft on the date of the event is presented in Figure 7, indicating a quadrature configuration of the Earth and both the spacecraft. It should be noted that the two parts of the jet had different velocities. The results suggest, besides gravity of the Sun, that the confinement of coronal magnetic field is another crucial factor affecting the jet structure and consequently the observed velocities. From *SDO*/AIA 171 Å images associated with Figure 9, the confinement of coronal magnetic field played a leading role to decelerate the velocity from 350 km s^{-1} to 190 km s^{-1}. Hence, the confinement of coronal magnetic field also resulted in the jet bifurcated two parts (front part and bottom part). The video (video9) was made using *SDO*/AIA 171 Å difference images, indicating the arch-like shape of the front part, while the entire front part of the jet looked like a bubble. The forefront of the bubble appears like water waves with a 190 km s^{-1} moving forward. Hence, different from the *SDO* angle of view, from the *STEREO* COR1 angle of view we could observe the bubble-like CME, namely, the bubble-like CME being the front part of the jet. It suggested that, from video 6, the bubble-like CME and the jet-like CME they were so close and the configuration was different from observing by *SDO*. The reason might be that the satellites have difference angle of views. From *SDO* angle of view, the jet projection on the disk of the Sun looked like a Baseball Bat. But from *STEREO* viewing angle, the jet-like CME looked like a candle flame, and very near the bubble-like CME. The double CMEs, in our work, are overlapped, due to the angle of view. We could clearly recognize the jet from *SDO* in seven EUV wavelength channels, though only three channels are reported in our paper. Interestingly, we could follow the jet eruption process projection on the disk of the Sun. In Shen et al. (2012) work, however, the jet eruption was almost vertical to the Sun (from the *SDO* view). In their work, the double CMEs were side by side, and not clearly distinguishable, different from our double-CME being easily noticeable. A further noted difference is the jet-like and bubble-like CMEs, in this paper, showing an overlapped part; d) the active area appears undoubtedly more complex than the Shen et al. (2012) event. In fact, before 21:35 UT, the active area was subject of multiple jets. Based on our analysis, especially of the *BBSO* images, we conclude that the filament has emerged after the recurrent jet eruptions. This characteristic appears to be the main difference from the work of Shen et al. (2012). When the jets erupted, the filament emerged with intense untwisted motion accompanied with series of intense flares reaching, from 22:05 UT to 22:12 UT, M-class level. This characteristic indeed is considered as the third principle difference compared to Shen et al. (2012) event. Nevertheless the two double-CME events also show some similarities, such as the occurrence of jet eruptions followed by filament eruption and flare. We believe our double-CME event is undoubtedly more significant for future and more wide investigations. Certainly in the future, other similar simultaneous double CMEs or possibly even simultaneous three or more than three CMEs will be observed. Recently, various papers have dealt with studies presenting jet or blowout-jet and one- or double-CME, such as Chen et al. (2015), Alzate & Morgan (2016), Liu et al. (2015). In contrast to the cited studies, our jet eruption event present different and peculiar aspects:1) the blowout jet eruption produced a short time shock wave, this maybe the first event to be observed. 2) the jet was a large-scale solar activity and accompanied by a double-CME; 3) in contrast to the model presented in Liu et al. (2015), two successive CME eruptions with a vertical orientation nature, did not occur simultaneously; 4) Alzate & Morgan (2016) presented jet eruptions area followed by a slow CME type. Simultaneous double-CME seems appears thus to be not frequently observed and a rare phenomena, which strongly makes them, together with simultaneous multiple-CME (MCMEs: more than two CMEs), a possible hot topic in solar astrophysics research.

Due to high-spatial and high-temporal resolution multi-wavelength observations from two different angle of views, we successfully identify the second double-CME event. Combining the analysis Figure 2, Figure 6 and Figure 9, we present a cartoon (Figure 10)to interpret the physical mechanism of the coronal blowout jet, and the associated jet-like CME and the bubble-like CME. Shibata et al. (1992) presented a standard X-ray jet model, and Moore et al. (2010) further proposed the standard jet model and the blowout jet model. Moore et al. (2010) pointed out that about two thirds fit the standard coronal jets and about one third were another type. From Moore et al. (2010), the authors presented a model for blowout jets. The model was more complex than the standard jets model. Moore et al. (2015) pointed out that the essential difference between the standard jets and the blowout jets was that the magnetic field inside bash arch. It should be noted that

the standard jet was only produced by a burst of interchange reconnection of the outside, while the interior bash arch remains closed. A blowout jet, in contrast, was generated by a blowout eruption of the interior field of the bash arch. The authors also pointed out that a standard jet had not enough free energy to produce a CME. On the contrary, a blowout jet had enough free energy to produce a CME. Thanks to the more reconnection in the interior of the bash arch in a blowout jet, the blowout jet was easily to be heated and brighten in EUV and X-ray emission during the eruptive growth phase. In addition, due to the complex field in the interior of the bash arch in a blowout jet, as the bash arch drove more widespread interchange reconnection, generating more open field with jet outflow on the them, and led to the blowout jet spray wider and wider. A standard jet had no these characteristics. Shen et al. (2012) presented a cartoon to demonstrate the coronal blowout jet with simultaneous CMEs. Interestingly, the bubble-like CME and jet-like CME were side by side from *STEREO* view point. However, it is unfortunate that the event was too faint to distinguish. In our paper, we present the cartoon to demonstrate the second double-CME event. Interestingly, our blowout jet has a large scale, and the bubble-like CME and jet-like CME are overlapping from COR1 Ahead and COR1 Bhead of *STEREO* view points. Thanks to the *SDO*/AIA high-spatial and high-temporal resolution multi-wavelength images, we can clearly to observe the blowout jet and easily to distinguish the bubble. In addition, by seeing the movies of nine wavelength bands and 171 Å , 193 Å were made from difference images (video10, video9 and video4). Combining Moore et al. (2015) and Sterling et al. (2015), we present the Figure 10 to demonstrate the second double-CME event, which came from a blowout jet eruption. Our schematic neatly demonstrates the trigger mechanism of the double-CME. Moore et al. (2013), from *SDO*/AIA 304 Å movies, revealed that there was a spinning motion in the eruptive growth phase in most of the larger X-ray jets. The cool component was easily to observed by the *SDO*/AIA 304 Å images. We also observed a discernible spinning motion from 22:05 UT to 22:15 UT by seeing the video2 during the "F" rising period (a time-elapse movie of various wavelength bands). The spinning motion is very easy to be seen from this movie. In our schematic Figure 10 panel (a) and panel (b), we display the untwisting motion and the direction of the rotation. In Shen et al. (2012), the authors presented a cartoon to display the process of the first double-CME event. There was a pity they did not display the untwisting motion in their schematic. We think the two simultaneous bubble-like CME and jet-like CME events have a significance for the solar physics. We hope that more and more similar events to be observed in the future. From this paper present event, we have a bold prediction, the three-CME event may be observed in the future, two jet-like CMEs and a bubble-like CME. We conceive that another open field on the right of the closed field, and closed field reconnection with open fields on the two sides. The two jet-like CMEs maybe have a early or late ordinal. These results are highly encouraging for further future observational campaign-efforts and modeling investigations, particularly in understanding the driving physical mechanisms (variety of important physical parameters) behind the nature of jet eruptive solar events and their close association with coronal jets or/and filament eruptions.

4. ACKNOWLEDGEMENT

This work was supported by grants from NSFC (11078004, 11533009), and from the Key Laboratory of Geospace Environment, CAS, University of Science & Technology of China. AE is partly supported by CAS Fellowships for young international scientists, grant 2012Y1JA0002. The research by the KSU astronomy unit-A. Elmhamdi and A.S. Kordi- was supported by King Saud University, Dearship of Scientific Research, College of Science Research Center.

REFERENCES

Adams, M., Sterling, A. C., Moore, R. L., et al. 2014, ApJ, 783, 11

Alzate, N. , & Morgan, H. 2016, ApJ, 823,129

Antiochos, S. K., DeVore, C. R., & Klimchuk, J. A. 1999, ApJ, 510, 485

Chen, J., Su, J. T., Yin, Z. Q., et al. 2015, ApJ, 815,71

Cirtain, J. W., Golub, L., Lundquist, L., et al. 2007, Science, 318, 1580

Dissauer, K., Temmer, M., Veronig, A., M., et al. 2016, ApJ, 830, 92

Filippov, B., Martsenyuk, O., Srivastava, A. K., & Uddin, W. 2015, MNRAS, 1117, 1129

Katsukawa, Y., Berger, T. E., Ichimoto, K., et al. 2007, Science, 318, 1594

Kayshap, P., Abhishek, K. S, & K. M. 2013, ApJ, 763, 24

Li, X. H., Yang, S. H., Chen, H. D., et al. 2015, ApJL, 814, L13

Lin, J., & Forbes, T. G. 2000, J. Geophys. Res., 105, 2375

Liu, Y. D., Hu, H. D., Zhu, B., et al. 2017, ApJ, 834, 158

Liu, C., Deng, N., Liu, R., et al. 2011, ApJL, 735, L18

Liu, J. J., Wang, Y. M., Shen, C. L., et al. 2015,ApJ, 813, 115

Liu, Y. & Kurokawa, H. 2004, ApJ, 610, 1136

Liu, Y., Kurokawa, H., Kitai, R., et al. 2005, SoPh, 228, 149

Liu, Y. 2008, SoPh, 249, 75

Madjarska, M. S., Wiegelmann, T. 2009, ApJ, 701,253

Morton, R. J., Srivastava, A. K., & Erdélyi, R. 2012, A&A, 542,A70
Moore, R. L., Cirtain, J. W., Sterling, A. C., et al. 2010, ApJ, 720,757
Moore, R. L., Sterling, A. C., Falconer, et al. 2013, ApJ, 769, 134
Moore, R. L., Sterling, A. C., Falconer, et al. 2015, ApJ, 806, 11
Mou, C. Z., Huang, Z. H., Xia, L. D., et al. 2016, ApJ, 818,9
Murawski, K., Srivastava, A. K., Zaqarashvili, T. V. 2011, A&A, 535, A58
Muhr, N., Veronig, A. M., Kienreich, I. W., et al. 2014, SoPh, 289, 4563
Scherrer, P. H., Schou, J., Bush, R. I., et al. 2012, SoPh, 275, 207
Shen, Y. D., Liu, Y., Su, J. T., et al. 2011, ApJL, 735, L43
Shen,Y. D.,Liu,Y., Su, J. T., et al. 2012, ApJ, 745,164
Shibata, K., & Uchida, Y. 1986, SoPh, 103, 299
Shibata, K., Ishido, Y., Acton, L. W., et al. 1992, PASJ, 44, L173
Sterling, A. C., & Moore, R. L. 2004, ApJ, 613, 1221
Sterling, A. C, Moore, R. L., Falconer, D. A., & Adams, M., 2015, Nature, 523, 437
Sterling, A. C., Moore, R. L., Falconer, D. A., et al. 2016, ApJ, 821, 100
Shimojo, M., Hashimoto, S., Shibata, K., et al. 1996, PASJ, 48, 123
Shimojo, M., Shibata, K., & Harvey, K. L. 1998, SoPh, 178, 379
Zhang, Q. M., Li, D., Ning, Z. J., et al. 2016, ApJ, 827:27

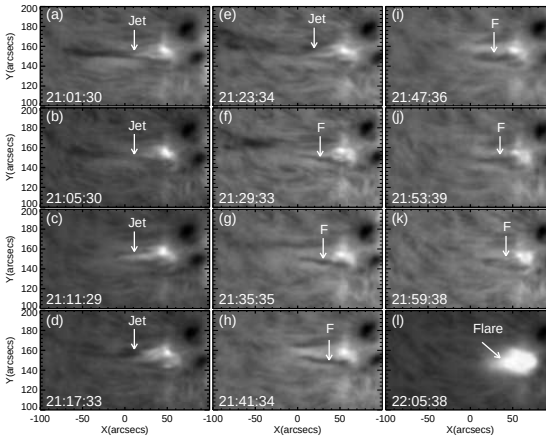

Figure 1. A sequence of *BBSO* Hα images covering the filament formation episode, and the series of blowout jet eruptions occurring just before 22:05 UT. Panels (a) to (e) indicates the "Jet" location, from 21:01 UT to 21:59 UT, highlight the main stage of the filament formation. Panel (l) reports the filament eruption, and the production of the C9.4 flare. After several blowout jet ejections, a small filament develops at the ejection activity area. It appears that around 22:05 UT the small filament started to eject, when we can notice activity area begins to brighten (see video1).

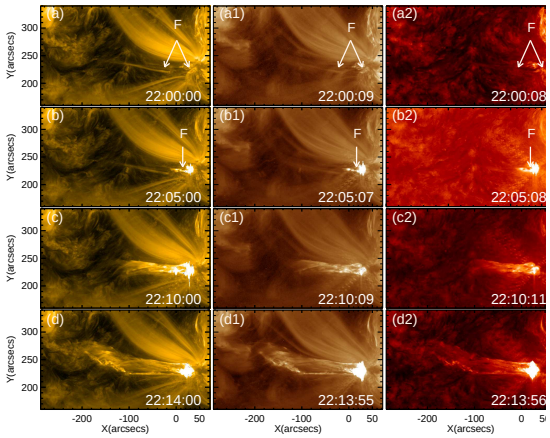

Figure 2. SDO multi-wavelength images at 171 Å , 193 Å , and 304 Å , highlighting the jet eruption development. We could clearly see the filament at the top panel at 22:00 UT. At 22:05 UT the filament started to erupt, followed by the cooling and dimming processes (second panel; (b) to (b2)). From (c) to (c2), the jet growed larger than before, and had an obvious untwist motion. At about 22:20 UT the jet appears to split into two parts, with the front part starting to move on (i.e. the jet-like CME and bubble-like CME; video2; available in the accompanying online material).

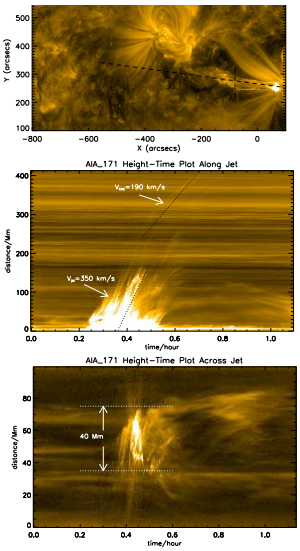

Figure 3. The Distance - Time plot from the cross-cut along the jet with AIA 171 Å image shows in top image. The black dotted lines indicates the trend along the jet. The first part velocity is estimated to be about 350 km s^{-1} (bottom half), while the second part velocity is about 190 km s^{-1} (the upper part). The result of the height-time plots are reported in the bottom figure, where we measured the jet width (brighter area) to be zt least 40 Mm, indicating the very largr jet scale. A simple linear fit is adopted in our computations.

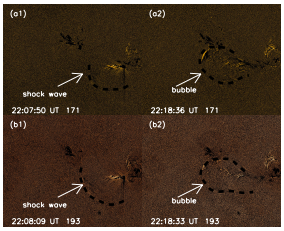

Figure 4. Using 171 Å and 193 Å difference images. Panels (a1) and (b1) showed the profile of the shock wave with white arrows and doted lines. Panels (a2) and (b2) showed the bubble-like CME and jet-like CME at the beginning of the jet eruption (see video3). The arched lines indicated the bubble-like CME (see video4)

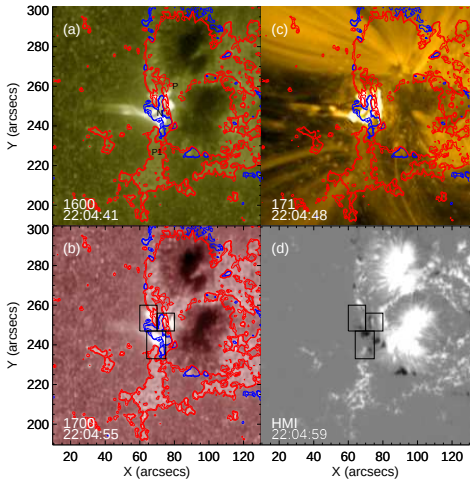

Figure 5. *SDO* 1600 Å , 1700 Å , 171 Å , and line-of-sight HMI images. Panels (a) to (c) report the HMI image overlaying AIA images at 22:04:59 UT. The blue line represents the negative magnetic field and red line represents the positive magnetic field. The contour levels are ±100, ±50 G. In panel (a), the labels "P", "N", "P1" indicate the main positive magnetic field, emerging negative magnetic field and the open positive magnetic field, respectively. Panel (b) highlights three bright points: " A1", " A2", " A3" , which are counterpart of panel (d). Panel (c) reports the jet eruption at the beginning stage. Panel (d) shows the line-of-sight HMI image and three magnetic regions of sizes: $5'' \times 11''$ " A1", $10'' \times 9''$ " A2", $11'' \times 14''$ " A3".

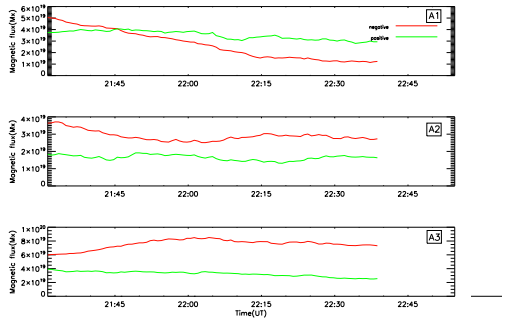

Figure 6. The magnetic flux evolution curves. The three panels, from top to bottom, correspond to " A1", " A2", " A3" regions of Figure 5 panel (d), respectively. The red line represents the negative magnetic flux, while the green line shows the positive magnetic flux. The rapid decline in the negative flux, top panel, might be considered as indicative for magnetic cancellation leading role in " A1". The middle panel illustrates the decrease and the increase of the negative flux of " A2"area. The bottom panel highlights the increase phase, 21:31 UT to 22:05 UT, and the almost negative flux plateau stage, 22:05 UT to 22:30 UT, for " A3" region.

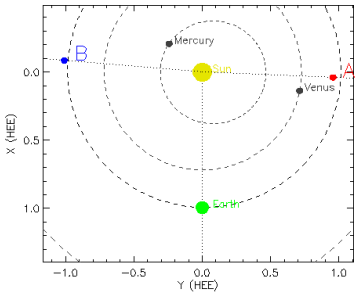

Figure 7. The positions of *STEREO* two satellites and earth at 22:10 UT, in the field of view (FOV) of the COR1 Ahead and COR1 Bhead of *STEREO*. Because the position of earth, COR1 Ahead and COR1 Bhead are very perfect, and fortunately have successfully imaged the blowout jet eruption (video5).

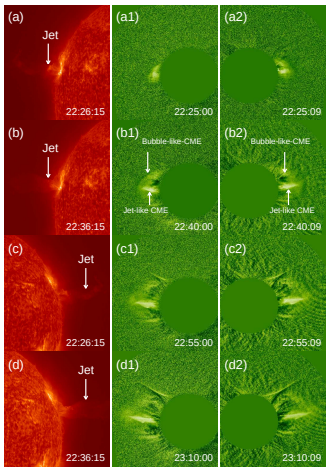

Figure 8. Panels (a) and (b) correspond to *STEREO* Ahead 304 Å images, (c) and (d) are *STEREO* Bhead 304 Å images. The second and the third columns show, respectively, the simultaneous COR1 Ahead and COR1 Bhead difference images of *STEREO*. Panel (b1) and (b2) highlight the jet-like CME and bubble-like CME shape geometry. The white arrows indicate the jet-like CME as well as the bubble-like CME profiles, with a very clear associated are-like feature. More details can be seen in the available accompanying online material (video6; video7,video8).

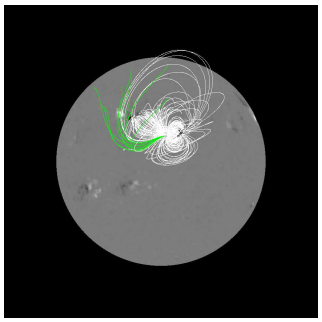

Figure 9. A full-disk line-of-sight magnetogram and corresponding magnetic topology structure of AR NOAA 11166. The green line represents open magnetic field and the white line represents the closed field, respectively. In Figure 9 shows a magnetic field extrapolation obtained using the Potential Field Source Surface (PFSS), a full-disk line-of-sight magnetogram and corresponding magnetic topology structure of AR NOAA 11166. as deduced by applying a potential-field source-surface (PFSS) extrapola- tion to the observed photospheric field. The green line represents open magnetic field and the white line represents the closed field, respectively.

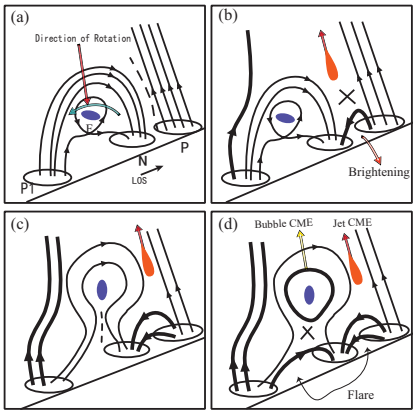

Figure 10. The proposed cartoon-model demonstrating the coronal jet and the associated simultaneous CMEs. (a) the initial magnetic configuration. (b) the external reconnection and the generated jet-like CME. (c) the new current sheet beneath " F" displaying an untwisting motion and reconnection. (d) the internal reconnection and the production of the bubble-like CME. The dashed lines indicate the current sheets, while the thick continuous lines represent the reconnected field lines. The X symbols were representation of reconnection sites.